

Semileptonic $B \rightarrow \pi$ Decays from an Omnès Improved Nonrelativistic Constituent Quark Model.

C. Albertus,¹ J.M. Flynn,² E. Hernández,³ J. Nieves,¹ and J.M. Verde-Velasco³

¹*Departamento de Física Moderna, Universidad de Granada, E-18071 Granada, Spain.*

²*School of Physics & Astronomy, University of Southampton, Southampton SO17 1BJ, UK*

³*Grupo de Física Nuclear, Facultad de Ciencias, E-37008 Salamanca, Spain.*

The semileptonic $B \rightarrow \pi l^+ \nu_l$ decay is studied starting from a simple quark model which includes the influence of the B^* pole. To extend the predictions of a nonrelativistic constituent quark model from its region of applicability near $q_{\max}^2 = (m_B - m_\pi)^2$ to all q^2 values accessible in the physical decay, we use a novel multiply-subtracted Omnès dispersion relation, which considerably diminishes the form factor dependence on the elastic $\pi B \rightarrow \pi B$ scattering amplitudes at high energies. By comparison to the experimental branching fraction we extract $|V_{ub}| = 0.0034 \pm 0.0003$ (exp) ± 0.0007 (theory). To further test our framework, we also study $D \rightarrow \pi$ and $D \rightarrow K$ decays and find excellent results $\frac{f_\pi^+(0)}{f_K^+(0)} = 0.80 \pm 0.03$, $\frac{\mathcal{B}(D^0 \rightarrow \pi^- e^+ \nu_e)}{\mathcal{B}(D^0 \rightarrow K^- e^+ \nu_e)} = 0.079 \pm 0.008$. In particular for the $D \rightarrow \pi$ case, we reproduce, with high accuracy, the three-flavor lattice QCD results recently obtained by the Fermilab-MILC-HPQCD Collaboration. While for the $D \rightarrow K$ case, we successfully describe the data for $f^+(q^2)/f^+(0)$ recently measured by the FOCUS Collaboration.

PACS numbers: 12.15.Hh, 12.39.Jh, 11.55.Fv, 13.20.He, 13.20.Fc

I. INTRODUCTION

Exclusive semileptonic decays of B -mesons are of great interest, since they can be used to determine the Cabibbo-Kobayashi-Maskawa (CKM) matrix elements $|V_{ub}|$ and $|V_{cb}|$. In the latter case, heavy quark symmetry greatly simplifies the theoretical understanding of the hadronic transition matrix elements and thus the overall theoretical uncertainty on the decay process is under control [1]. The measurement of the exclusive semileptonic decay $B \rightarrow \pi l^+ \nu_l$ by the CLEO Collaboration [2, 3] can be used to determine the CKM parameter $|V_{ub}|$. This exclusive method provides an important alternative to the extraction of $|V_{ub}|$ from inclusive measurements of $B \rightarrow X_u l^+ \nu_l$. For semileptonic decays of charmed or bottom mesons into light mesons there are no flavor symmetries to constrain the hadronic matrix elements, and as a result, the errors on $|V_{ub}|$ are currently dominated¹ by theoretical uncertainties [1]. An accurate determination of $|V_{ub}|$ with well-understood uncertainties remains one of the fundamental priorities for heavy flavor physics.

The transition amplitude for the exclusive semileptonic $b \rightarrow u$ decays factorizes into leptonic and hadronic parts. The hadronic matrix elements contain the non-perturbative, strong-interaction effects and have been extensively evaluated within different approaches. Thus, several lattice QCD (first in the quenched approximation, [4, 5, 6, 7, 8, 9], and more recently using dynamical configurations [10, 11]), light-cone sum rule (LCSR) [12, 13, 14, 15, 16] and constituent quark model [17, 18, 19, 20, 21, 22, 23, 24, 25] calculations have been carried out in recent years. Each of the above methods has only a limited range of applicability, namely: LCSR are suitable for describing the low squared momentum transfer (q^2) region of the form factors, while Lattice QCD, because of the limitation on the magnitude of spatial momentum components, provides results only for the high q^2 region. Constituent quark models may give the form factors in the full q^2 range, but they are not closely related to the QCD Lagrangian² and therefore have input parameters which are not directly measurable and might not be of fundamental significance. Thus, it is evident that a combination of various methods is required.

Watson's theorem for the $B \rightarrow \pi l^+ \nu_l$ process allows one to write a dispersion relation for each of the form factors entering in the hadronic matrix element. This procedure leads to the so-called Omnès representation [26], which can be used to constrain the q^2 dependence of the form factors from the elastic $\pi B \rightarrow \pi B$ scattering amplitudes [27]. In Ref. [27], once-subtracted dispersion relations were used, and though promising results were found, they suffered from sizeable uncertainties because of imprecise knowledge of the $\pi B \rightarrow \pi B$ phase shifts far from threshold. A recent re-analysis of the Omnès representation in this context [28], has shown that the use of multiply-subtracted dispersion relations considerably diminishes the form factor dependence on the elastic $\pi B \rightarrow \pi B$ scattering amplitudes at high

¹ The current best value for $|V_{cd}|$ comes from neutrino production of charm off valence d quarks (with the cross section from perturbative QCD), rather than from semileptonic D decays.

² A rigorous derivation of this approach as an effective theory of QCD in the non-perturbative regime has not been obtained.

energies, and more importantly points out that the Omnès representation of the form factors can be used to combine predictions from various methods in different q^2 regions.

In this paper we study the semileptonic $B \rightarrow \pi l^+ \nu_l$ decay. We take advantage of the findings of Ref. [28] and use the predictions of LCSR calculations at $q^2 = 0$ to extend the predictions of a simple nonrelativistic constituent quark model (NRCQM) from its region of applicability (near $q_{\max}^2 = (m_B - m_\pi)^2$) to all q^2 values accessible in the physical decay. We also use the available lattice QCD data to test our approach. We use a Monte Carlo procedure to find theoretical error bands for the form factors and the decay width. From our estimate of the decay width and the branching ratio measurement of Ref. [3] we obtain

$$|V_{ub}|_{\text{this work}} = 0.0034 \pm 0.0003 (\text{exp}) \pm 0.0007 (\text{theory}) \quad (1)$$

To further test this simple framework, we also study the $D \rightarrow \pi$ and $D \rightarrow K$ decays, for which there exist precise experimental data and for which the relevant CKM matrix elements ($|V_{cd}|$ and $|V_{cs}|$) are also well known. We find

$$f_\pi^+(0) = 0.63 \pm 0.02, \quad f_K^+(0) = 0.79 \pm 0.01, \quad \frac{f_\pi^+(0)}{f_K^+(0)} = 0.80 \pm 0.03, \quad \frac{\mathcal{B}(D^0 \rightarrow \pi^- e^+ \nu_e)}{\mathcal{B}(D^0 \rightarrow K^- e^+ \nu_e)} \Big|_{\text{this work}} = 0.079 \pm 0.008 \quad (2)$$

The plan of this paper is as follows. After this introduction, we study the semileptonic $B \rightarrow \pi$ decay in Sect. II. First we set up the form factor decomposition (Subsect. II A), discuss the valence quark approximation (Subsect. II B) and the role played by the B^* resonance (Subsect. II C). The Omnès dispersion relation and its application to this decay is addressed in Subsect. II D and in the Appendix. Finally, in Subsect. II E we use our framework to determine $|V_{ub}|$, paying special attention to estimating the uncertainties of the determination. In Sect. III we study the $D \rightarrow \pi$ and $D \rightarrow K$ semileptonic decays and finally in Sect. IV we present our conclusions.

II. SEMILEPTONIC $B \rightarrow \pi$ DECAYS

A. Differential Decay Width and Form Factor Decomposition

Using Lorentz, parity, and time-reversal invariance, the matrix element for the semileptonic $B^0 \rightarrow \pi^- l^+ \nu_l$ decay can be parametrized in terms of two invariant and dimensionless form factors as³

$$\langle \pi(p_\pi) | V^\mu | B(p_B) \rangle = \left(p_B + p_\pi - q \frac{m_B^2 - m_\pi^2}{q^2} \right)^\mu f^+(q^2) + q^\mu \frac{m_B^2 - m_\pi^2}{q^2} f^0(q^2) \quad (3)$$

where $q^\mu = (p_B - p_\pi)^\mu$ is the four momentum transfer and $m_B = 5279.4$ MeV and $m_\pi = 139.57$ MeV are the B^0 and π^- masses, respectively. The physical meaning of the form factors is clear in the helicity basis, in which f^+ (f^0) corresponds to a transition amplitude with 1^- (0^+) spin-parity quantum numbers in the center of mass of the lepton pair. For massless leptons ($l = e$ or μ), the total decay rate is given by

$$\Gamma(B^0 \rightarrow \pi^- l^+ \nu_l) = \frac{G_F^2 |V_{ub}|^2}{192 \pi^3 m_B^3} \int_0^{q_{\max}^2} dq^2 [\lambda(q^2)]^{\frac{3}{2}} |f^+(q^2)|^2 \quad (4)$$

with $q_{\max}^2 = (m_B - m_\pi)^2$, $G_F = 1.16637 \times 10^{-5}$ GeV⁻² and $\lambda(q^2) = (m_B^2 + m_\pi^2 - q^2)^2 - 4m_B^2 m_\pi^2 = 4m_B^2 |\vec{p}_\pi|^2$, with \vec{p}_π the pion three-momentum in the B rest frame.

Measurements of the B^0 lifetime, $\tau_{B^0} = (1.536 \pm 0.014) \times 10^{-12}$ s and of the $B^0 \rightarrow \pi^- l^+ \nu_l$ branching fraction, $\mathcal{B}_{\text{exp}}(B^0 \rightarrow \pi^- l^+ \nu_l) = (1.33 \pm 0.22) \times 10^{-4}$ [1] lead to

$$\Gamma_{\text{exp}}(B^0 \rightarrow \pi^- l^+ \nu_l) = (8.7 \pm 1.5) \times 10^7 \text{ s}^{-1} = (5.7 \pm 1.0) \times 10^{-14} \text{ MeV}, \quad l = e \text{ or } \mu \quad (5)$$

B. Nonrelativistic Constituent Quark Model: Valence Quark Contribution

Within the spectator approximation, considering only the valence quark contribution and assuming that the B and π mesons are S -wave quark-antiquark bound states, a NRCQM (with constituent quark masses m_b and $m_l = m_u = m_d$)

³ Note that the axial current does not contribute to transitions between pseudoscalar mesons.

predicts [29]:

$$\frac{\langle \pi(E_\pi, -\vec{q}) | V^\mu | B(m_B, \vec{0}) \rangle^{\text{val}}}{\sqrt{4m_B E_\pi}} = \int \frac{d^3l}{4\pi} \sqrt{\frac{E_b(\vec{l}) + m_b}{2E_b(\vec{l})}} \sqrt{\frac{E_u(\vec{l} + \vec{q}) + m_u}{2E_u(\vec{l} + \vec{q})}} \phi_{\text{rel}}^B(|\vec{l}|) \phi_{\text{rel}}^\pi(|\vec{l} + \frac{m_{sp}}{m_u + m_{sp}} \vec{q}|) \mathcal{V}^\mu(\vec{l}, \vec{q})$$

$$\mathcal{V}^\mu(\vec{l}, \vec{q}) = \begin{pmatrix} 1 + \frac{\vec{l}^2 + \vec{l} \cdot \vec{q}}{(E_b(\vec{l}) + m_b)(E_u(\vec{l} + \vec{q}) + m_u)} \\ -\frac{\vec{l}}{E_b(\vec{l}) + m_b} - \frac{\vec{l} + \vec{q}}{E_u(\vec{l} + \vec{q}) + m_u} \end{pmatrix} \quad (6)$$

with $E_\pi = \sqrt{m_\pi^2 + \vec{q}^2}$, $E_{b,u}(\vec{k}) = \sqrt{m_{b,u}^2 + \vec{k}^2}$, m_{sp} the spectator quark mass (m_d in this case) and $\phi_{\text{rel}}^{B,\pi}(k)$ the Fourier transforms of the radial coordinate space B, π meson wave functions, which describe the relative dynamics of the quark-antiquark pair⁴.

To evaluate the coordinate space wave function we have used several nonrelativistic quark-antiquark interactions. Their general structure is as follows [30, 31]

$$V_{ij}^{q\bar{q}}(r) = -\frac{\kappa(1 - e^{-r/r_c})}{r} + \lambda r^p - \Lambda + \left\{ a_0 \frac{\kappa}{m_i m_j} \frac{e^{-r/r_0}}{r r_0^2} + \frac{2\pi}{3m_i m_j} \kappa' (1 - e^{-r/r_c}) \frac{e^{-r^2/x_0^2}}{\pi^{\frac{3}{2}} x_0^3} \right\} \vec{\sigma}_i \vec{\sigma}_j \quad (7)$$

with $\vec{\sigma}$ the spin Pauli matrices, m_i the constituent quark masses and

$$x_0(m_i, m_j) = A \left(\frac{2m_i m_j}{m_i + m_j} \right)^{-B} \quad (8)$$

The potentials considered differ in the form factors used for the hyperfine terms, the power of the confining term ($p = 1$, as suggested by lattice QCD calculations [32], or $p = 2/3$ which gives the correct asymptotic Regge trajectories for mesons [33]), or the use of a form factor in the one gluon exchange Coulomb potential. All interactions have been adjusted to reproduce the light (π, ρ, K, K^* , etc.) and heavy-light (D, D^*, B, B^* , etc.) meson spectra and lead to precise predictions for the charmed and bottom baryon ($\Lambda_{c,b}, \Sigma_{c,b}, \Sigma_{c,b}^*, \Xi_{c,b}, \Xi_{c,b}', \Xi_{c,b}^*, \Omega_{c,b}$ and $\Omega_{c,b}^*$) masses [31, 34] and for the semileptonic $\Lambda_b^0 \rightarrow \Lambda_c^+ l^- \bar{\nu}_l$ and $\Xi_b^0 \rightarrow \Xi_c^+ l^- \bar{\nu}_l$ [35] decays.

Typical NRCQM valence quark predictions for the f^+ and f^0 form factors are depicted in Fig. 1. The AL1 potential from Ref. [31] has been used⁵ and for comparison quenched lattice results are also plotted. Preliminary unquenched lattice calculations have been presented recently [10, 11], but no significant difference between quenched and unquenched calculations is observed [36], within relatively large statistical errors. In addition, LCSR provide accurate and theoretically well founded results in the $q^2 = 0$ region. Thus, we have a LCSR value [13]

$$\text{LCSR} : f^+(0) = 0.28 \pm 0.05 \quad (9)$$

which is also plotted in Fig. 1.

Fig. 1 clearly shows the deficiencies of the NRCQM valence quark description of the $B \rightarrow \pi l^+ \nu_l$ semileptonic decay. It fails over the full range of q^2 values. Close to q_{max}^2 , where the nonrelativistic Schrödinger equation should work best, the influence of the B^* resonance is clearly visible [19]. At the opposite end, close to $q^2 = 0$, where $|\vec{q}| \approx 2.5$ GeV, predictions from a nonrelativistic scheme are clearly not trustworthy. As a result, a value for the width $\Gamma_{\text{NRCQM}}^{\text{val}}(B^0 \rightarrow \pi^- l^+ \nu_l) = 2.4 \left(\frac{|V_{ub}|}{0.0032} \right)^2 \times 10^{-14}$ MeV is obtained, which is around a factor of two smaller than the CLEO measurement quoted in Eq. (5).

C. Nonrelativistic Constituent Quark Model: B^* Resonance Contribution

A NRCQM description of the decay process should be feasible in the neighborhood of q_{max}^2 . Indeed, this is the case for the semileptonic $B \rightarrow D l \bar{\nu}_l$ and $B \rightarrow D^* l \bar{\nu}_l$ decays, recently studied in Ref. [29] with the same NRCQM as here.

⁴ They are normalized to $\int_0^{+\infty} dk k^2 |\phi_{\text{rel}}^{B,\pi}(k)|^2 = 1$

⁵ The sensitivity of the results to the quark-antiquark nonrelativistic interaction will be discussed in detail later.

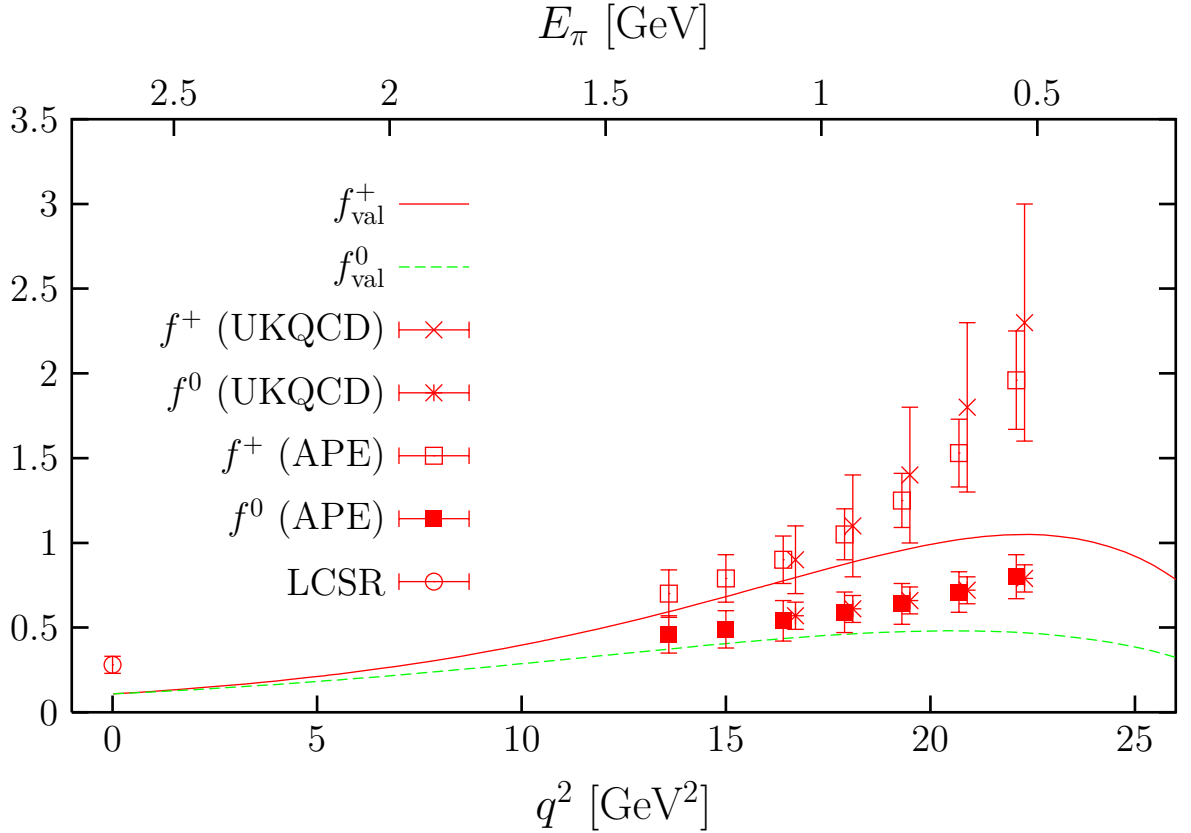


FIG. 1: NRCQM valence quark f^+ and f^0 form factors from the AL1 inter-quark interaction [31]. Lattice data points are taken from Refs. [7] (UKQCD) and [8] (APE) and the LCSR estimate at $q^2 = 0$ is given in Ref. [13].

The difference here is that, as first pointed out in Ref. [19], in the chiral limit and as $m_b \rightarrow \infty$, the decay $B^0 \rightarrow \pi^- l^+ \nu_l$ should be dominated near zero pion recoil by the effects of the B^* resonance, which is quite close to q_{max}^2 . In the picture of Ref. [19], the one we will adopt here, the B^* contribution plays a role only near q_{max}^2 , since it is strongly suppressed by a soft hadronic vertex. This is in sharp contrast to phenomenological parameterizations of f^+ which assume it dominates over the full range accessible in the physical decay [4]. The B^* effects of the type considered here are not dual to the valence quark model form factors and must be added as a distinct coherent contribution to heavy quark decay near q_{max}^2 [19]. We will focus on the f^+ form factor, which determines the decay width for massless leptons, and we evaluate the contribution to it from the diagram depicted in Fig. 2. It leads to a hadronic amplitude (normalizations as in Ref. [29])

$$-iT^\mu = -i\hat{g}_{B^*B\pi}(q^2)p_\pi^\nu \left(i\frac{-g_\nu^\mu + q^\mu q_\nu/m_{B^*}^2}{q^2 - m_{B^*}^2} \right) i\sqrt{q^2}\hat{f}_{B^*}(q^2) \quad (10)$$

with $m_{B^*} = 5325$ MeV, and \hat{f}_{B^*} and $\hat{g}_{B^*B\pi}$ the B^* decay constant and the strong $B^*B\pi$ dimensionless coupling

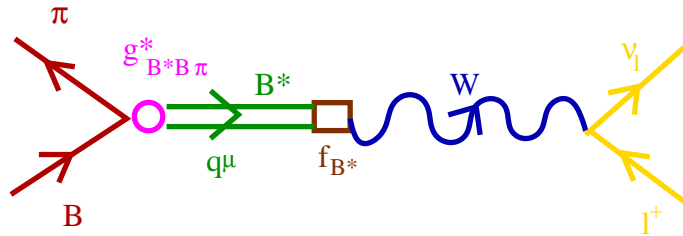


FIG. 2: B^* resonance contribution to the f^+ form factor for the semileptonic $B \rightarrow \pi$ decay.

constant for a virtual B^* meson, respectively. On the B^* mass shell, the hadron matrix elements $\hat{f}_{B^*}(q^2 = m_{B^*}^2) \equiv f_{B^*}$

and $\widehat{g}_{B^*B\pi}(q^2 = m_{B^*}^2) \equiv g_{B^*B\pi}$ reduce to the ordinary B^* decay constant and coupling of a pion to B and B^* mesons. The latter is related, in the heavy quark limit, to \widehat{g} , the coupling of the vector and pseudoscalar heavy-light mesons to the pion [37, 38]⁶

$$g_{B^*B\pi} = \left(\frac{2\widehat{g}\sqrt{m_B m_{B^*}}}{f_\pi} \right) (1 + \mathcal{O}(1/m_b)) \quad (11)$$

From Eq. (10) we get

$$f_{\text{pole}}^+(q^2) = \frac{1}{2} \widehat{g}_{B^*B\pi}(q^2) \frac{\sqrt{q^2} \widehat{f}_{B^*}(q^2)}{m_{B^*}^2 - q^2} \quad (12)$$

There is no direct experimental determination of $g_{B^*B\pi}$, because there is no phase space for the decay $B^* \rightarrow B\pi$. The available experimental results for $D^* \rightarrow D\pi$ [1] can be related to $g_{B^*B\pi}$, through heavy quark symmetry. There is no direct measurements of f_{B^*} either. In Ref. [29] we computed, within the same NRCQM approach as the one outlined here, both $g_{B^*B\pi}$ and f_{B^*} , and we found a value of 9.1 ± 0.9 GeV for the product of both quantities, which appears in f_{pole}^+ at $q^2 = m_{B^*}^2$. Lattice QCD simulations have measured f_{B^*} [39] and $g_{B^*B\pi}$ [40] to be

$$f_{B^*} = 190 \pm 30 \text{ MeV} \quad g_{B^*B\pi} = 47 \pm 5 \pm 8 \Rightarrow [g_{B^*B\pi} f_{B^*}]_{\text{Latt-QCD}} = 8.9 \pm 2.2 \text{ GeV} \quad (13)$$

where we have added errors in quadrature. Thus the lattice prediction for the product $g_{B^*B\pi} f_{B^*}$ is in remarkable agreement, within 3%, with our NRCQM estimate in [29]. In what follows we will use the value and error for the product estimated from the lattice data and use the NRCQM of Ref. [29] to determine the q^2 dependence of $\widehat{g}_{B^*B\pi}(q^2)$ and $\widehat{f}_{B^*}(q^2)$, as we will discuss below. There are other recent estimates for $g_{B^*B\pi}$ ([41, 42]) and f_{B^*} ([43]), but given the existing uncertainties, all of them are compatible with the lattice values quoted in Eq. (13).

As mentioned above, we use the NRCQM framework to estimate the q^2 dependence of the product of $\widehat{f}_{B^*}(q^2) \widehat{g}_{B^*B\pi}(q^2)$. Since the NRCQM always uses on-shell meson wave functions, all q^2 dependence will arise from the kinematical factors relating the quark model matrix elements and the hadron form factors. For instance, from Eq. (13) of Ref. [29] we find a rather mild q^2 dependence

$$\widehat{f}_{B^*}(q^2) \sqrt[4]{q^2} = f_{B^*} \sqrt{m_{B^*}} \quad (14)$$

In the same manner, we use Eqs. (50) and (51) of Ref. [29] to determine the q^2 dependence of $\widehat{g}_{B^*B\pi}$, setting the B -meson four momentum $P^\mu = (m_B, \vec{P} = 0)$ and the B^* -meson four momentum $P^\mu = q^\mu = (m_B - E_\pi, \vec{P} = -\vec{q})$, and off-shell mass given by $\sqrt{q^2}$, $|\vec{q}| = \sqrt{E_\pi^2 - m_\pi^2}$, and E_π determined from q^2 as usual ($E_\pi = (m_B^2 + m_\pi^2 - q^2)/2m_B$). Thus, finally we evaluate

$$f_{\text{pole}}^+(q^2) = \frac{1}{2} G_{B^*}(q^2) \frac{\sqrt[4]{q^2}}{\sqrt{m_{B^*}}} \frac{m_{B^*} [g_{B^*B\pi} f_{B^*}]_{\text{Latt-QCD}}}{m_{B^*}^2 - q^2} \quad (15)$$

where $G_{B^*}(q^2) = \widehat{g}_{B^*B\pi}(q^2)/g_{B^*B\pi}$ is a dimensionless hadronic factor normalized to one at $q^2 = m_{B^*}^2$, which accounts for the q^2 dependence of $B \rightarrow B^*\pi$ amplitude. In Fig. 3, we show the influence of the B^* resonance within our NRCQM and compare our results to those obtained by Isgur and Wise from the gaussian constituent quark model of Refs. [18, 19]. Our model for the B^* contribution compares well to that of Ref. [19], though the latter decreases faster owing to the use of a harmonic oscillator basis. The inclusion of f_{pole}^+ clearly improves the simple valence quark contribution and leads to a reasonable description of the lattice data from q_{max}^2 down to q^2 values around 15 GeV^2 . The low q^2 region is still poorly described within the current model since relativistic corrections there should be large.

The hadronic amplitude of Eq. (10) also leads to a small contribution to the f^0 form factor. Though it also improves the description for the highest q^2 values, it is not large enough and it is necessary to consider the influence of the lightest 0^+ B -resonances [27] (for instance a resonance around 5660 MeV [44]).

D. Omnès Representation

Here we use the Omnès representation of the f^+ form factor to combine the NRCQM predictions at high q^2 values, say above 18 GeV^2 , with the LCSR result at $q^2 = 0$. In this way we obtain the full q^2 dependence of the form factor

⁶ We use the normalization $f_\pi \approx 131 \text{ MeV}$.

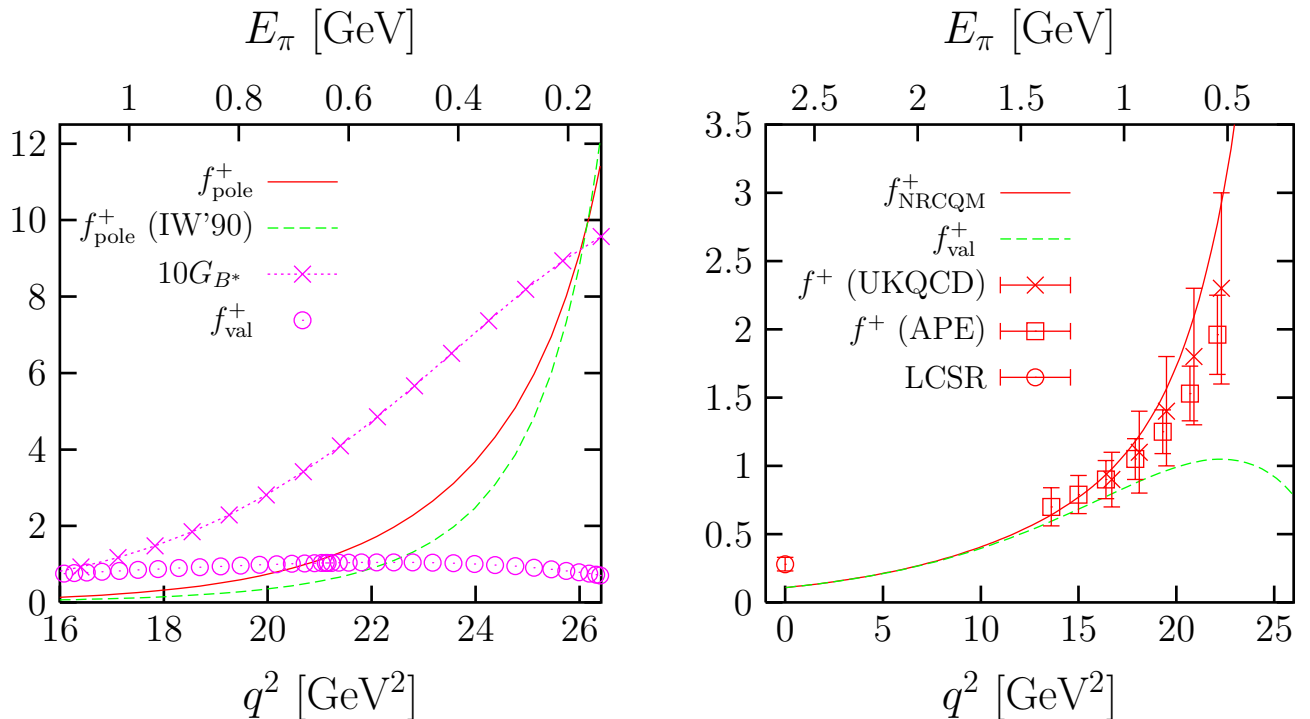


FIG. 3: **Left:** The solid line denotes the AL1 NRCQM B^* pole contribution to f^+ (Eq. (15)), while the dashed line stands for the B^* contribution to f^+ obtained within the gaussian constituent quark model of Refs. [18, 19]. We also plot the G_{B^*} hadron factor introduced in Eq. (15) and the valence quark contribution to f^+ depicted in Fig. 1. **Right:** Valence quark and valence quark plus B^* -pole (denoted as NRCQM) contributions to f^+ . We also plot lattice QCD and LCSR f^+ data from the same references as in Fig. 1.

and thus can determine the $|V_{ub}|$ CKM matrix element from the integrated semileptonic width. As shown in the Appendix, the $(n+1)$ -subtracted Omnès representation for f^+ reads:

$$\begin{aligned}
 f^+(q^2) &= \left(\prod_{j=0}^n [f^+(q_j^2)]^{\alpha_j(q^2)} \right) \exp \left\{ \mathcal{I}_\delta(q^2; q_0^2, q_1^2, \dots, q_n^2) \prod_{k=0}^n (q^2 - q_k^2) \right\}, \\
 \mathcal{I}_\delta(q^2; q_0^2, \dots, q_n^2) &= \frac{1}{\pi} \int_{s_{\text{th}}}^{+\infty} \frac{ds}{(s - q_0^2) \cdots (s - q_n^2)} \frac{\delta(s)}{s - q^2}, \\
 \alpha_j(q^2) &= \prod_{j \neq k=0}^n \frac{q^2 - q_k^2}{q_j^2 - q_k^2},
 \end{aligned} \tag{16}$$

with $q^2 < s_{\text{th}} = (m_B + m_\pi)^2$ and $q_0^2, \dots, q_n^2 \in]-\infty, s_{\text{th}}[$. This representation requires as an input the elastic $\pi B \rightarrow \pi B$ phase shift $\delta(s)$ in the $J^P = 1^-$ and isospin $I = 1/2$ channel plus the form-factor at $(n+1)$ q^2 -values ($q_0^2, q_1^2, \dots, q_n^2$) below the πB threshold.

We would like to stress that from a theoretical point of view the Omnès representation is derived from first principles: the well-established Mandelstam hypothesis [45] of maximum analyticity and Watson's theorem [46]

$$\frac{f^+(s + i\epsilon)}{f^+(s - i\epsilon)} = \frac{T(s + i\epsilon)}{T(s - i\epsilon)} = e^{2i\delta(s)}, \quad s > s_{\text{th}}, \quad T(s) = \frac{8\pi i s}{\lambda^{\frac{1}{2}}(s)} \left(e^{2i\delta(s)} - 1 \right) \tag{17}$$

Omnès ideas have been used successfully to account for final state interactions in kaon decays [48]⁷ and in Ref. [27], a once-subtracted Omnès representation (subtraction point $q_0^2 = 0$) was applied to the study of semi-leptonic $B \rightarrow \pi$

⁷ There, however, multiple derivatives evaluated at a single point are used as input instead of subtractions for different q^2 values.

decays. In the latter work phase shifts were evaluated by solving the Bethe-Salpeter equation in the so-called *on-shell scheme* [49], with a kernel determined by the direct tree level amplitude from the lowest order heavy meson chiral perturbation theory lagrangian [38], together with the tree diagrams for B^* exchange which involve the leading interaction with coupling \hat{g} . Such a model accommodates the B^* as a πB bound state and should acceptably describe phase shifts close to threshold. It led to promising results for f^+ [27], but theoretical uncertainties on the form factor were not negligible, since to compute the Omnès factor \mathcal{I}_δ (Eq. (16)) requires elastic phase-shifts far from threshold⁸. To include the effects of higher resonances on $\delta(s)$ requires input of the masses and couplings of such resonances. We therefore make many subtractions in the Omnès dispersion relation to suppress the impact of $\delta(s)$ at large s . This will leave a systematic effect in our results, but this should be less than that coming from the NRCQM plus B^* pole used as our main input.

As the number of subtractions increases the integration region relevant in Eq. (16) gets reduced and, if this number is large enough, only the phase shifts at or near threshold will be needed. Note that close to threshold the p -wave phase shift behaves as

$$\delta(s) = n_b \pi - p^3 a + \dots \quad (18)$$

where n_b is the number of bound states in the channel (Levinson's theorem [47]), p is the πB center of mass momentum and a the corresponding scattering volume. In our case $n_b = 1$ if we consider the B^* as a πB bound state. Here, we will perform a large number of subtractions so that approximating $\delta(s) \approx \pi$ in Eq. (16) will be justified. The Omnès factor \mathcal{I}_δ can then be evaluated analytically and we find for $q^2 < s_{\text{th}}$

$$f^+(q^2) \approx \frac{1}{s_{\text{th}} - q^2} \prod_{j=0}^n [f^+(q_j^2)(s_{\text{th}} - q_j^2)]^{\alpha_j(q^2)}, \quad n \gg 1 \quad (19)$$

Next we use the above formula to combine the LCSR result at $q^2 = 0$ and those obtained from our NRCQM in the high q^2 region and presented in the previous section. Thus we have used the f^+ NRCQM (valence + pole) predictions for five q^2 values ranging from q_{max}^2 down⁹ to about 18 GeV²:

$$(q^2/\text{GeV}^2, f^+(q^2)) = \begin{cases} (23.574, 4.1373), \\ (21.804, 2.5821), \\ (21.116, 2.1969), \\ (20.173, 1.7916), \\ (18.290, 1.2591) \end{cases} \quad (20)$$

together with the LCSR result of Eq. (9) at $q^2 = 0$. When one uses a large number of subtractions, as is the case here, the α_j exponents become large and there are huge cancellations (note the normalization condition given in Eq. (A7)). This is the reason why above, and to ensure numerical stability, we have quoted five significant digits for the NRCQM input. We are aware that uncertainties are larger than a precision of five digits, and we will carefully take this fact into account below. Results are shown in Fig. 4. As can be seen there, we obtain a simultaneous description of both lattice data in the high q^2 region and the LCSR prediction at $q^2 = 0$. In this way, starting from a nonrelativistic valence quark picture of the semileptonic process (Subsect. IIB) with all its obvious limitations, we have ended up with a realistic description of the relevant form factor for all q^2 values accessible in the physical decay.

A final remark concerns the use of the simplified Omnès representation of Eq. (19) instead of the exact one of Eq. (16). For instance, if we use five subtractions (we drop the NRCQM point at $q^2 = 21.1$ GeV²) and the full Omnès representation¹⁰ of Eq. (16), we find tiny differences from the results shown in Fig. 4. These differences are negligible (below 1%) above 10 GeV², and though larger, still quite small (around 5-7% at most in the 5 GeV² region) below 10 GeV².

⁸ Higher resonance effects on phase shifts cannot be neglected far from threshold. In particular the LCSR result at $q^2 = 0$ hints that at least an extra $J^P = 1^-$ resonance, located around 6 GeV, has to be included in the once-subtracted Omnès relation scheme [27].

⁹ From Eq. (6), we see that the arguments of the meson wave function are $|\vec{l}|$ and $|\vec{l} + \vec{q}/2|$. For $q^2 = 18$ GeV², half of the transferred momentum, $|\vec{q}|/2$, is about 0.4–0.5 GeV, which is of the same order as $(\vec{l}^2)_{\phi_{B,\pi}}^{\frac{1}{2}}$. Since the non-relativistic quark-antiquark interactions, $V(r)$, have been adjusted to reproduce the meson binding energies, they effectively incorporate some relativistic corrections and hence one might expect this effective nonrelativistic framework to provide reasonable meson wave functions for momenta of order $(\vec{l}^2)_{\phi_{B,\pi}}^{\frac{1}{2}}$.

This could explain why the NRCQM describes the lattice data (right panel of Fig. 3) from high values of q^2 down to values of q^2 even smaller than 18 GeV². Nevertheless, we find it surprising that the nonrelativistic constituent quark model works as well as it does [20].

¹⁰ We use the model of Ref. [27] to obtain the phase-shifts.

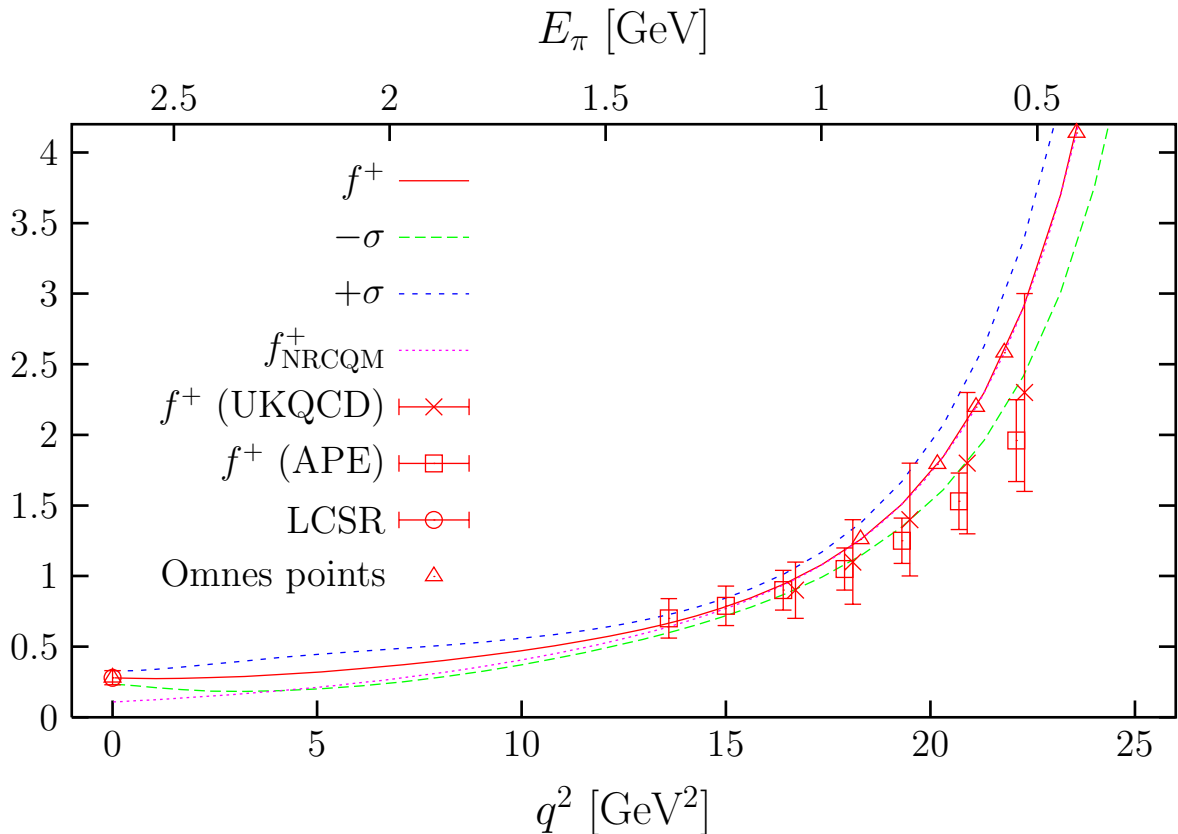


FIG. 4: Solid line: f^+ form factor from a 6-subtracted Omnès representation, Eq. (19). Triangles denote the input subtraction points of the Omnès dispersion relation (five points obtained from our AL1 NRCQM plus the Ref. [13] LCSR result at $q^2 = 0$). Lattice data are from Refs. [7](UKQCD) and [8](APE), and the AL1 valence quark plus B^* -pole contribution to f^+ is also shown (denoted f_{NRCQM}^+). Finally, $\pm\sigma$ lines show the theoretical uncertainty bands on the Omnès form factor inherited from the errors in Eq. (13) and from the quark-antiquark interaction model dependence (see Subsect.IIE for details).

E. Determination of $|V_{ub}|$: Error Analysis

The CKM element $|V_{ub}|$ can be determined by comparing the experimental decay width (Eq. (5)) with the result of performing the phase space integration of Eq. (4) using the form factor f^+ determined in the previous subsection. Here, we will pay special attention to estimating the theoretical uncertainties. We have two main sources of theoretical errors:

1. *Uncertainties in the constituent quark-antiquark nonrelativistic interaction:* To estimate those, we will evaluate the spread of integrated widths obtained when five different potentials (AL1, AL2, AP1, AP2 and BD, in the notation of Ref. [31]) are considered. The forms and main characteristics of those potentials were discussed in Eqs. (7) and (8). As mentioned in Subsect. IIB, all interactions have been adjusted to reproduce the light and heavy-light meson spectra and lead to precise predictions for the charmed and bottom baryon masses [31] and for the semileptonic $\Lambda_b^0 \rightarrow \Lambda_c^+ l^- \bar{\nu}_l$ and $\Xi_b^0 \rightarrow \Xi_c^+ l^- \bar{\nu}_l$ [35] decays.
2. *Uncertainties on $[g_{B^*B\pi}f_{B^*}]$ and on the input to the multiply-subtracted Omnès representation:* Errors on $[g_{B^*B\pi}f_{B^*}]$, quoted in Eq. (13), affect the B^* pole contribution to f^+ (see Eq. (15)) and also induce uncertainties in the NRCQM prediction for the five points used as input to the Omnès representation in Eq. (19). Quark-antiquark potential uncertainties, discussed in the previous item, also induce uncertainties in the Omnès input. The errors on the $q^2 = 0$ data point (LCSR), quoted in Eq. (9), should also be taken into account.

To take these uncertainties into account, we proceed in two steps:

1. We fix the quark-antiquark potential to the AL1 interaction as in all previous subsections. By means of a Monte

Carlo simulation, we generate a total of 1000 ($[g_{B^*B\pi}f_{B^*}]_{\text{Latt-QCD}}, f^+(0)_{\text{LCSR}}$) pairs¹¹ from an uncorrelated two dimensional gaussian distribution, with central values and standard deviations taken from Eqs. (13) and (9), respectively. For each of the 1000 pairs we build up the six points that we use in our Omnès scheme (Eq. (19)) and thus find 1000 different determinations of f^+ over the whole q^2 range accessible in the $B \rightarrow \pi$ decay. For each value of q^2 , we discard the highest and lowest 16% of the values obtained for the form factor, to leave a 68% confidence level band which forms part of the theoretical uncertainty shown in Fig. 4. Since the output distributions are not gaussian in general, this accounts for possible skewness.

Performing the phase space integration for each of the 1000 form factor samples and again discarding the highest and lowest 16% of the values, we find

$$\frac{\Gamma(B^0 \rightarrow \pi^- l^+ \nu_l)}{|V_{ub}|^2} = (0.50_{-0.10}^{+0.14}) \times 10^{-8} \text{ MeV} \quad (21)$$

2. We fix the ($[g_{B^*B\pi}f_{B^*}]_{\text{Latt-QCD}}, f^+(0)_{\text{LCSR}}$) pair to their central values and compute the decay width with each of the five quark-antiquark interactions discussed above. From the spread of output values, we find

$$\frac{\Gamma(B^0 \rightarrow \pi^- l^+ \nu_l)}{|V_{ub}|^2} = (0.50 \pm 0.15) \times 10^{-8} \text{ MeV} \quad (22)$$

Adding both sources of error in quadrature, we get

$$\frac{\Gamma(B^0 \rightarrow \pi^- l^+ \nu_l)}{|V_{ub}|^2} = (0.50 \pm 0.20) \times 10^{-8} \text{ MeV} \quad (23)$$

and comparing to the measurement of the width in Eq. (5) we find

$$|V_{ub}|_{\text{this work}} = 0.0034 \pm 0.0003 (\text{exp}) \pm 0.0007 (\text{theory}) \quad (24)$$

The CLEO Collaboration [3] obtains from studies of the $B^0 \rightarrow \pi^- l^+ \nu_l$ branching fraction and q^2 distributions, using LCSR for $0 \leq q^2 < 16 \text{ GeV}^2$ and lattice QCD for $16 \text{ GeV}^2 \leq q^2 < q_{\text{max}}^2$,

$$|V_{ub}|_{\text{CLEO}} = 0.0032 \pm 0.0003 (\text{exp})_{-0.0004}^{+0.0006} (\text{theory}) \quad (25)$$

We see that both determinations of $|V_{ub}|$ are in an excellent agreement and that in both cases the error is dominated by uncertainties in the theoretical treatment. We have also calculated partially integrated branching ratios,

$$\mathcal{B}(q_1^2 \leq q^2 < q_2^2) = \frac{\mathcal{B}_{\text{exp}}^{\text{total}}(B^0 \rightarrow \pi^- l^+ \nu_l)}{\Gamma} \int_{q_1^2}^{q_2^2} dq^2 \frac{d\Gamma}{dq^2} \quad (26)$$

Theoretical uncertainties partially cancel in the ratio $\int_{q_1^2}^{q_2^2} dq^2 \frac{d\Gamma}{dq^2} / \Gamma$. Our results are compiled in the Table I. There it can be seen that they compare reasonably well with those quoted in Ref. [3].

	$B^0 \rightarrow \pi^- l^+ \nu_l$		
	$\mathcal{B}(0 \leq q^2 < 8 \text{ GeV}^2)/10^{-5}$	$\mathcal{B}(8 \leq q^2 < 16 \text{ GeV}^2)/10^{-5}$	$\mathcal{B}(q^2 \geq 16 \text{ GeV}^2)/10^{-5}$
CLEO [3]	4.3 ± 1.2	6.5 ± 1.3	2.5 ± 1.0
This work	$4.3 \pm 0.7 [\text{exp}] \pm 1.2 [\text{theory}]$	$4.1 \pm 0.7 [\text{exp}] \pm 0.4 [\text{theory}]$	$4.9 \pm 0.8 [\text{exp}] \pm 1.2 [\text{theory}]$

TABLE I: Partially integrated branching ratios (see Eq. (26)).

Finally, at each value of q^2 we also compute the spread of values obtained for the f^+ form factor when the five different quark-antiquark interactions are used. This procedure gives us a further theoretical error on $f^+(q^2)$ at fixed q^2 and by adding it in quadrature to that obtained previously from uncertainties on the ($[g_{B^*B\pi}f_{B^*}]_{\text{Latt-QCD}}, f^+(0)_{\text{LCSR}}$) pair, we determine the theoretical error bands shown in Fig. 4.

¹¹ We have checked that the errors quoted in the following are already stable when 500 event simulations are performed.

III. SEMILEPTONIC $D \rightarrow \pi$ AND $D \rightarrow K$ DECAYS

As a further test of our predictions for the $B \rightarrow \pi$ semileptonic process, we present results for the $D \rightarrow \pi$ and $D \rightarrow K$ decays for which there are precise experimental data [1]:

$$\mathcal{B}_{\text{exp}}(D^0 \rightarrow \pi^- e^+ \nu_e) = (3.6 \pm 0.6) \times 10^{-3}, \quad \Gamma_{\text{exp}}(D^0 \rightarrow \pi^- e^+ \nu_e) = (5.8 \pm 1.0) \times 10^{-12} \text{ MeV} \quad (27)$$

$$\mathcal{B}_{\text{exp}}(D^0 \rightarrow K^- e^+ \nu_e) = (3.58 \pm 0.18) \times 10^{-2}, \quad \Gamma_{\text{exp}}(D^0 \rightarrow K^- e^+ \nu_e) = (57 \pm 3) \times 10^{-12} \text{ MeV}, \quad (28)$$

with life time $\tau_{D^0} = (410.3 \pm 1.5) \times 10^{-15} \text{ s}$ and $|V_{cd}| = 0.224 \pm 0.003$, $|V_{cs}| = 0.9737 \pm 0.0007$.

In the last two years there has been renewed interest in these decays. The first three-flavor lattice QCD results [50] have appeared, superseding the old quenched ones [8, 9, 51], and the BES [52] and CLEO [53] collaborations have new measurements of the branching ratios

$$\text{BES} : \mathcal{B}(D^0 \rightarrow \pi^- e^+ \nu_e) = (3.3 \pm 1.3) \times 10^{-3}, \quad \mathcal{B}(D^0 \rightarrow K^- e^+ \nu_e) = (3.8 \pm 0.5) \times 10^{-2} \quad (29)$$

$$\text{CLEO} : \frac{\mathcal{B}(D^0 \rightarrow \pi^- e^+ \nu_e)}{\mathcal{B}(D^0 \rightarrow K^- e^+ \nu_e)} = 0.082 \pm 0.006 \pm 0.005 \quad (30)$$

Both collaborations have also determined the form factor at $q^2 = 0$

$$\text{BES} : f_{\pi}^+(0) = 0.73 \pm 0.14 \pm 0.06, \quad f_{K}^+(0) = 0.78 \pm 0.04 \pm 0.03, \quad \frac{f_{\pi}^+(0)}{f_{K}^+(0)} = 0.93 \pm 0.19 \pm 0.07 \quad (31)$$

$$\text{CLEO} : \frac{f_{\pi}^+(0)}{f_{K}^+(0)} = 0.86 \pm 0.07_{-0.04}^{+0.06} \pm 0.01 \quad (32)$$

In the following we will apply the NRCQM developed for the $B \rightarrow \pi$ decay to the description of these D -meson semileptonic transitions. All formulae of Sect. II can be used here with the obvious replacements: $B \rightarrow D, B^* \rightarrow D^*$ for the $D^0 \rightarrow \pi^- l^+ \nu_l$ process, and $B \rightarrow D, \pi \rightarrow K, B^* \rightarrow D_s^*$ for the $D^0 \rightarrow K^- l^+ \nu_l$ process. We will use $m_{D^0} = 1864.6 \text{ MeV}$, $m_{D^*} = 2010 \text{ MeV}$, $m_{D_s^*} = 2112.1 \text{ MeV}$ and $m_{K^-} = 493.68 \text{ MeV}$.

A. $D \rightarrow \pi l \bar{\nu}_l$

Since there is phase space for the $D^* \rightarrow D\pi$ decay to occur, the $g_{D^*D\pi}$ hadronic constant has been experimentally measured (CLEO [54])

$$g_{D^*D\pi} = 17.9 \pm 0.3 \pm 1.9 \quad (33)$$

Taking $f_{D^*} = (234 \pm 20) \text{ MeV}$ from Ref. [39], we find¹²

$$[g_{D^*D\pi} f_{D^*}]_{\text{Exp-Latt}} = 4.2 \pm 0.6 \text{ GeV} \quad (34)$$

where we have added errors in quadrature. In Ref. [29] and using the same set of NRCQM's, we found a value of $4.9 \pm 0.5 \text{ GeV}$ for the above product, in reasonable agreement with Eq. (34). The value quoted in Eq. (34) determines the D^* -pole contribution, above $q^2 = 0$, to f^+ and adding it to the valence quark contribution we obtain the results shown in Fig. 5. We find excellent agreement between our description of the form factor and that provided by the unquenched lattice simulation of Ref. [50]. As can be seen in the figure, the D^* -pole contribution is dominant above $q^2 = 1.5 \text{ GeV}^2$ and it remains sizeable down to 0.5 GeV^2 . We do not see the need to Omnès improve the NRCQM description of the decay since it is quite good for the whole q^2 range. On the other hand, we see that the pion energy ranges from m_{π} up to about 1 GeV , which was also the maximum value for E_{π} in the five NRCQM data-points used in the subtracted Omnès representation for the semileptonic $B \rightarrow \pi$ decay depicted in Fig. 4. This reinforces our belief in the reliability of our determination of $|V_{ub}|$ presented in Subject. II E. Considering our theoretical uncertainties (errors on Eq. (34) and the spread of results obtained when different quark-antiquark interactions are considered) together with the experimental uncertainties on $|V_{cd}|$ quoted above, we find

$$\Gamma_{\text{this work}}(D^0 \rightarrow \pi^- e^+ \nu_e) = \left[5.2 \pm 0.1 (\text{exp} : |V_{cd}|) \pm 0.5 (\text{theory}) \right] \times 10^{-12} \text{ MeV} \quad (35)$$

¹² Note that the lattice QCD simulation of Ref. [55] measured $g_{D^*D\pi} = 18.8 \pm 2.3 \pm 2.0$ in good agreement with Eq. (33).

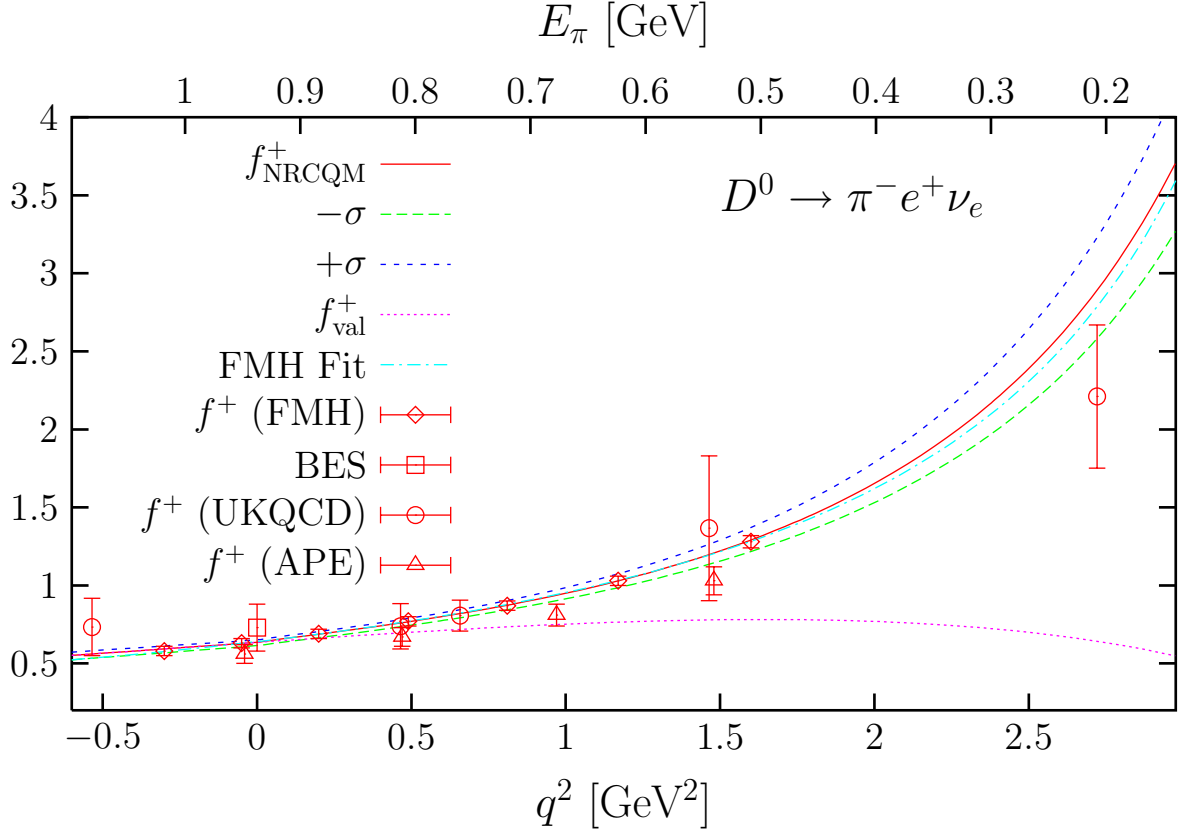


FIG. 5: Valence quark (dotted line) and valence quark plus D^* -pole (solid line denoted f_{NRCQM}^+) contributions to f^+ for $D \rightarrow \pi$ semileptonic decay. In both cases the AL1 quark-antiquark interaction has been used. Triangles ([8]) and circles ([51]) stand for the lattice QCD quenched results obtained by the APE and UKQCD Collaborations, respectively. We also plot the three-flavor lattice QCD results [50] from the Fermilab-MILC-HPQCD Collaboration (FMH, diamonds), the best fit (dash-dotted line) to this latter set of data-points (Eq. (5) of Ref. [50]), and the determination of f^+ at $q^2 = 0$ (square) by the BES Collaboration [52]. Finally, the $\pm\sigma$ lines stand for the theoretical uncertainty bands, inherited from the errors in Eq. (34) and from the quark-antiquark interaction model dependence.

in good agreement with Eq. (27). We also obtain

$$f_{\pi}^+(0) = 0.63 \pm 0.02 \quad (36)$$

compatible within errors with both the BES (0.73 ± 0.15) and the Fermilab-MILC-HPQCD (0.64 ± 0.07) results.

Finally in the left plot of Fig. 6, we compare the NRCQM predictions for the ratio $f^+(q^2)/f^+(0)$ with a pole form recently fitted to data by the FOCUS Collaboration [56].

B. $D \rightarrow Kl\bar{\nu}_l$

Since there is no phase space for the $D_s^* \rightarrow DK$ decay, we will estimate the $g_{D_s^*DK}$ coupling from the value quoted for $g_{D^*D\pi}$ in Eq. (33). The parameter \hat{g} defined in Eq. (11) describes the strong coupling of charmed mesons as well as of beauty mesons to the members of the octet of light pseudoscalars. We will assume flavor SU(3) symmetry for this basic quantity in the heavy quark chiral effective theory, and thus we will use [57]

$$g_{D_s^*DK} \approx \frac{2\hat{g}\sqrt{m_D m_{D_s^*}}}{f_K} \approx g_{D^*D\pi} \frac{\sqrt{m_{D_s^*}}}{\sqrt{m_{D^*}}} \frac{f_{\pi}}{f_K} \approx 15.3 \pm 1.6 \quad (37)$$

where we have taken $f_K/f_{\pi} \approx 1.2$ from Ref. [58], and have kept some SU(3) flavor breaking terms in the masses of the charmed vector mesons and in the kaon decay constant. Taking $f_{D_s^*} = (254 \pm 15)$ MeV from Ref. [39], we find

$$[g_{D_s^*DK} f_{D_s^*}]_{\text{SU(3)-Latt}} = 3.9 \pm 0.5 \text{ GeV} \quad (38)$$

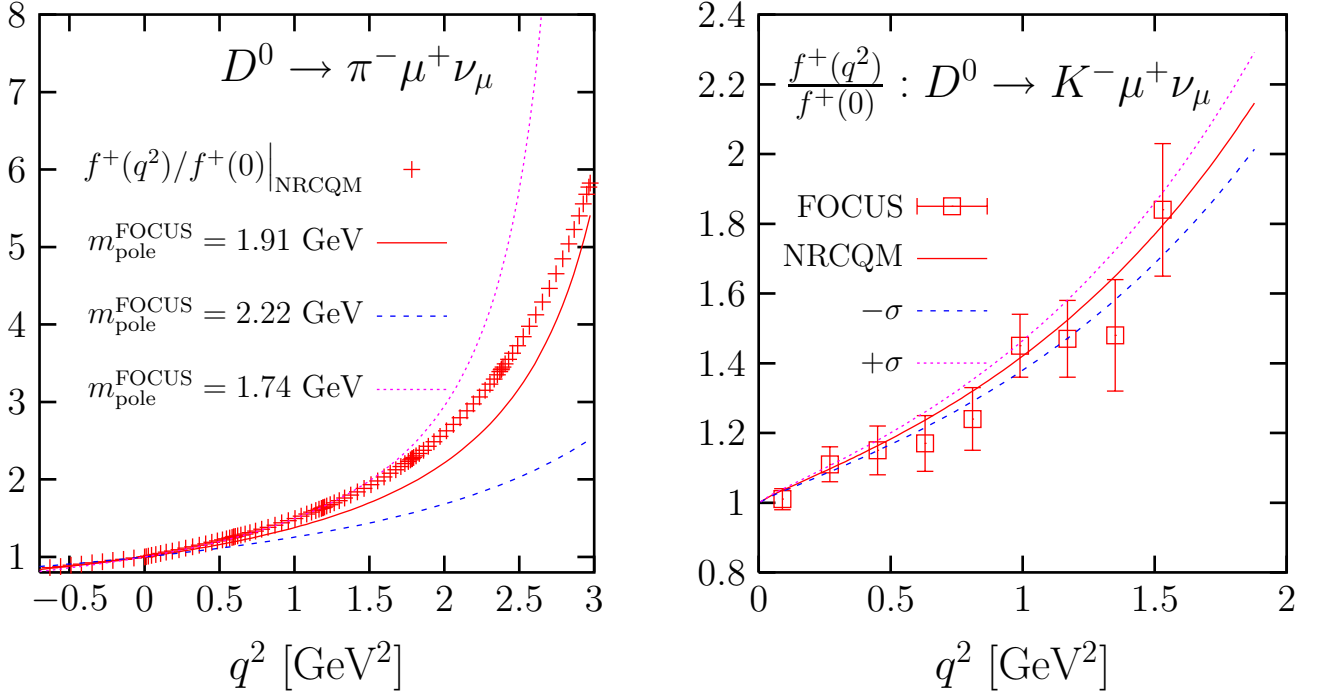


FIG. 6: NRCQM predictions for the ratio $f^+(q^2)/f^+(0)$ for both $D \rightarrow \pi$ (left) and $D \rightarrow K$ (right) semileptonic decays. For comparison we also plot experimental results from the FOCUS Collaboration [56]: pole fit for the $D \rightarrow \pi$ decay ($m_{\text{pole}} = 1.91^{+0.31}_{-0.17}$ GeV) and direct measurements of the form factor for different q^2 values, in the $D \rightarrow K$ case. In this latter case, the $\pm\sigma$ lines stand for our theoretical uncertainty bands, inherited from the errors in Eq. (34) and from the quark-antiquark interaction model dependence.

Our results for this decay are shown in Fig. 7. Several comments are in order:

1. We find reasonable agreement with the three-flavor lattice QCD results [50] up to kaon energies of the order of 1 GeV, which cover the whole q^2 range accessible in the physical decay. Discrepancies with lattice data are now more sizeable than in the $D \rightarrow \pi$ case and lattice unquenched data favor values for $[g_{D_s^* DK} f_{D_s^*}]_{\text{SU}(3)\text{-Latt}}$ smaller than the one used in our calculation (see Eq. (37)). Theoretical errors for f^+ are, in this case, mostly due to the uncertainties on $[g_{D_s^* DK} f_{D_s^*}]_{\text{SU}(3)\text{-Latt}}$. Nevertheless, we would like to point out that uncertainties on the value of $g_{D_s^* DK}$ might be larger than those quoted in Eq. (37), since flavor SU(3) corrections to the relation $g_{D_s^* DK} \approx 2\hat{g}\sqrt{m_D m_{D_s^*}}/f_K$ could be large ($m_s/m_c \gg m_{d,u}/m_c$).
2. The contribution of the vector resonance is less important than in the $B \rightarrow \pi$ and $D \rightarrow \pi$ decays, since the D_s^* is located relatively far from $\sqrt{q_{\text{max}}^2}$.
3. Our predictions for f^+ at negative values of q^2 , which do not enter into the phase space integral, suffer from larger uncertainties, since in that region the transferred momentum is larger than 1 GeV and, as for the $B \rightarrow \pi$ case, relativistic effects could become important. One could Omnès improve the NRCQM to achieve a better description of the form factor in the negative q^2 region.

In the right plot of Fig. 6, we compare the NRCQM predictions for the ratio $f^+(q^2)/f^+(0)$ with recently measured data from the FOCUS Collaboration [56] and find satisfactory and reassuring agreement.

For the integrated width, we find

$$\Gamma_{\text{this work}}(D^0 \rightarrow K^- e^+ \nu_e) = [66 \pm 3 \text{ (theory)}] \times 10^{-12} \text{ MeV} \quad (39)$$

which is about two standard deviations higher than the value quoted in Eq. (28).

Eqs. (27) and (28) lead to (adding errors in quadratures)

$$\frac{\mathcal{B}(D^0 \rightarrow \pi^- e^+ \nu_e)}{\mathcal{B}(D^0 \rightarrow K^- e^+ \nu_e)} = 0.101 \pm 0.017 \quad (40)$$

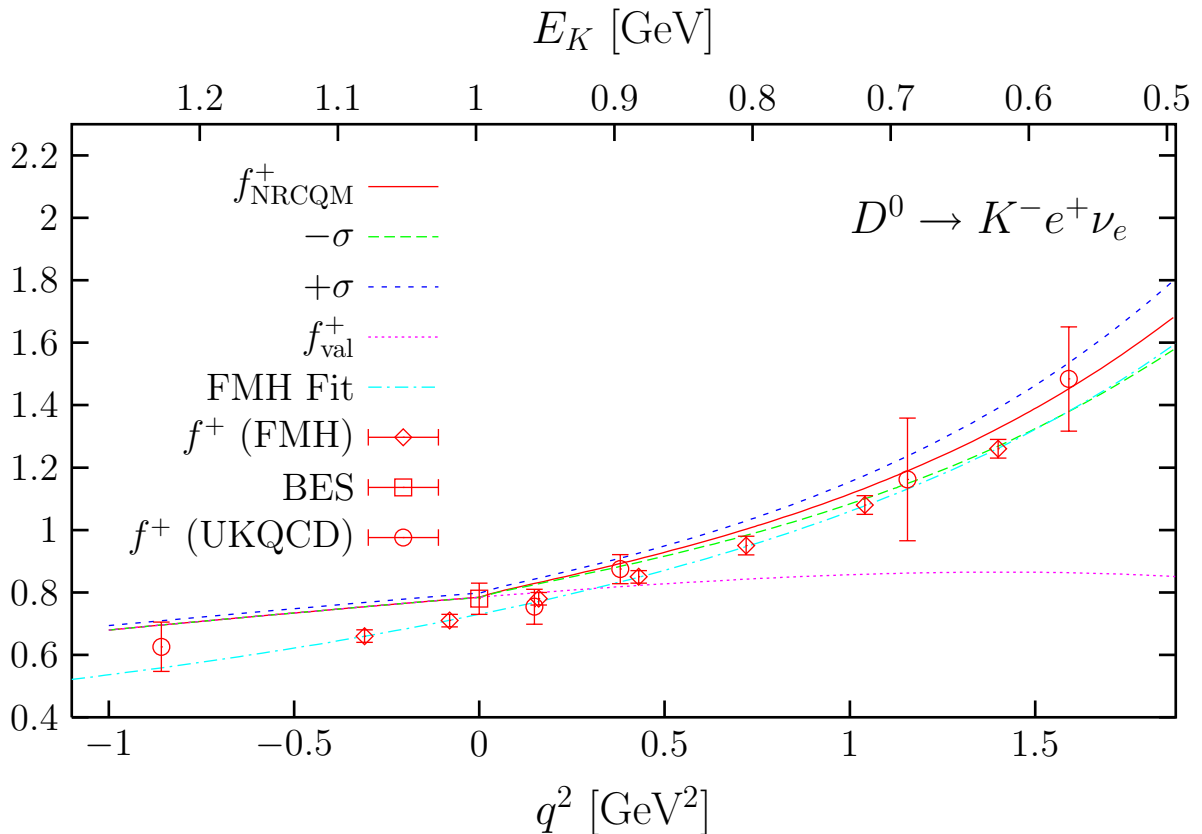


FIG. 7: Valence quark (dotted line) and valence quark plus D_s^* -pole (solid line denoted f_{NRCQM}^+) contributions to f^+ for $D \rightarrow K$ semileptonic decay. In both cases the AL1 quark-antiquark interaction has been used. Circles ([51]) and diamonds ([50]) stand for the lattice QCD quenched and unquenched results obtained by the UKQCD and the Fermilab-MILC-HPQCD Collaboration (labelled FMH), respectively. We also plot the best fit (dash-dotted line) to this latter set of data-points (Eq. (5) of Ref. [50]), and the determination of f^+ at $q^2 = 0$ (squared) by the BES Collaboration [52]. Finally, the $\pm\sigma$ lines stand for the theoretical uncertainty bands, inherited from the errors in Eq. (34) and from the quark-antiquark interaction model dependence.

which turns out to be a bit higher, though compatible within errors, than the recent CLEO determination quoted in Eq. (30). For this ratio of branching fractions we find

$$\frac{\mathcal{B}(D^0 \rightarrow \pi^- e^+ \nu_e)}{\mathcal{B}(D^0 \rightarrow K^- e^+ \nu_e)} \Big|_{\text{this work}} = 0.079 \pm 0.008 \quad (41)$$

in excellent agreement with the CLEO measurement. We also find

$$f_K^+(0) = 0.79 \pm 0.01, \quad \frac{f_\pi^+(0)}{f_K^+(0)} = 0.80 \pm 0.03 \quad (42)$$

which compare well to the recent experimental measurements in Eqs. (31) and (32).

IV. CONCLUDING REMARKS

We have shown the limitations of a valence quark model to describe the $B \rightarrow \pi$, $D \rightarrow \pi$ and $D \rightarrow K$ semileptonic decays. As a first correction, we have included in each case the heavy-light vector resonance pole contribution. For the semileptonic $B \rightarrow \pi$ decay, the inclusion of the B^* degree of freedom provides a realistic q^2 dependence of the relevant form factor, f^+ , from q_{max}^2 down to around 18 GeV^2 . We then use a multiply-subtracted Omnès dispersion relation, which considerably diminishes the form factor dependence on the elastic $\pi B \rightarrow \pi B$ scattering amplitudes at high energies, to combine LCSR results at $q^2 = 0$ with NRCQM predictions in the high q^2 region. As a result we have been able to predict the f^+ form factor for all q^2 values accessible in the physical decay. We

have used a Monte Carlo procedure and analyzed the predictions of five different quark-antiquark interactions to determine theoretical error bands for form factors and the decay width. This has allowed us to extract from the measured branching fraction the value $|V_{ub}| = 0.0034 \pm 0.0003$ (exp) ± 0.0007 (theory) in excellent agreement with the CLEO Collaboration determination of Ref. [3]. For the $D \rightarrow \pi$ semileptonic decay we have found excellent agreement between our model calculation (valence quark plus D^* -pole contributions) of f^+ and the one obtained by the unquenched lattice simulation of Ref. [50]. We found no need to Omnès-improve our calculation in this case. Our results $\Gamma(D^0 \rightarrow \pi^- e^+ \nu_e) = [5.2 \pm 0.1$ (exp $|V_{cd}|$) ± 0.5 (theory)] $\times 10^{-12}$ MeV and $f_\pi^+(0) = 0.63 \pm 0.02$ are in good agreement with experimental data. Finally for the $D \rightarrow K$ semileptonic decay we find good agreement, in the physical region, between our model calculation (valence quark plus D_s^* -pole contributions) of f^+ and lattice data, from UKQCD [51] and Fermilab-MILC-HPQCD [50], and also with recent measurements from the FOCUS Collaboration [56]. Again our results $\mathcal{B}(D^0 \rightarrow \pi^- e^+ \nu_e)/\mathcal{B}(D^0 \rightarrow K^- e^+ \nu_e) = 0.079 \pm 0.008$, $f_K^+(0) = 0.79 \pm 0.01$ and $f_\pi^+(0)/f_K^+(0) = 0.80 \pm 0.03$ are in good agreement with experimental determinations by the CLEO [53] and BES [52] Collaborations.

Acknowledgments

This research was supported by DGI and FEDER funds, under contracts BFM2002-03218, BFM2003-00856 and FPA2004-05616, by the Junta de Andalucía and Junta de Castilla y León under contracts FQM0225 and SA104/04, and it is part of the EU integrated infrastructure initiative Hadron Physics Project under contract number RII3-CT-2004-506078. C. Albertus wishes to acknowledge a grant from Junta de Andalucía. J.M. Verde-Velasco acknowledges a grant (AP2003-4147) from the Spanish Ministerio de Educación y Ciencia. J.M. Flynn acknowledges PPARC grant PPA/G/O/2002/00468, the hospitality of the Universidad de Granada and the Institute for Nuclear Theory at the University of Washington, and thanks the Department of Energy for partial support during the completion of this work.

APPENDIX A: MULTIPLY SUBTRACTED OMNÈS DISPERSION RELATION

Let the form factor¹³ $f^+(s)$ be analytic on the complex s plane (Mandelstam's hypothesis [45] of maximum analyticity) except for a cut $L \equiv [s_{\text{th}} = (m_B + m_\pi)^2, +\infty[$ along the real positive s axis, as demanded by Watson's theorem [46]. For real values $s < s_{\text{th}}$ the form factor is real which implies that the values of the form factor above and below the cut are complex conjugates of each other: $f^+(s + i\epsilon) = f^+(s - i\epsilon)^*$. For $s \geq s_{\text{th}}$, the form factor has a discontinuity across the cut and develops an imaginary part $f^+(s + i\epsilon) - f^+(s - i\epsilon) = 2i\text{Im}f(s + i\epsilon)$. Cauchy's theorem implies that $f^+(s)$ can be written as a dispersive integral along the cut and performing one subtraction at $s_0 < s_{\text{th}}$ one gets:

$$f^+(s) = f^+(s_0) + \frac{s - s_0}{\pi} \int_{s_{\text{th}}}^{+\infty} \frac{dx}{x - s_0} \frac{\text{Im}f^+(x)}{x - s}, \quad s \notin L, \quad s_0 < s_{\text{th}} \quad (\text{A1})$$

Depending on the asymptotic behavior of $f^+(s)$ at the extremes of the cut L , more subtractions may be needed to make the integral convergent. For the time being, let us assume that one subtraction is sufficient. The well known Omnès solution for the above dispersive representation is [26]:

$$O(s) = f^+(s_0) \exp \left\{ \frac{s - s_0}{\pi} \int_{s_{\text{th}}}^{+\infty} \frac{dx}{x - s_0} \frac{\delta(x)}{x - s} \right\}, \quad s \notin L, \quad s_0 < s_{\text{th}} \quad (\text{A2})$$

with $\delta(s)$ the elastic $\pi B \rightarrow \pi B$ phase shift¹⁴ in the $J^P = 1^-$ and isospin 1/2 channel (see Eq. (17)). $O(s)$ gives the physical form-factor since,

1. For $s \geq s_{\text{th}}$, we have

$$O(s \pm i\epsilon) = f^+(s_0) \exp \left\{ \frac{s - s_0}{\pi} \left[\mathcal{P} \int_{s_{\text{th}}}^{+\infty} \frac{dx}{x - s_0} \frac{\delta(x)}{x - s} \pm i\pi \frac{\delta(s)}{s - s_0} \right] \right\}$$

¹³ The discussion below can be trivially generalized to any scattering amplitude or form factor with definite total angular momentum and isospin quantum numbers.

¹⁴ Obviously $\delta(s)$ has to be defined as a continuous function of s .

$$= e^{\pm i\delta(s)} \left[f^+(s_0) \exp \left\{ \frac{s-s_0}{\pi} \mathcal{P} \int_{s_{\text{th}}}^{+\infty} \frac{dx}{x-s_0} \frac{\delta(x)}{x-s} \right\} \right] \quad (\text{A3})$$

where \mathcal{P} stands for principal part of the integral. Thus we have $O(s+i\epsilon) = O(s-i\epsilon)^*$, the function O is real for $s < s_{\text{th}}$ and has neither poles nor cuts, except for that required by Watson's theorem: $L \equiv [s_{\text{th}}, +\infty[$. The discontinuity across this cut is given by $O(s+i\epsilon) - O(s-i\epsilon) = 2i\text{Im}O(s+i\epsilon)$ and by construction $O(s_0) = f^+(s_0)$. Thus, both $f^+(s)$ and $O(s)$ satisfy the same dispersion relation (Eq. (A1)) and therefore both functions can differ at most by a polynomial with real coefficients, which should vanish at $s = s_0$. But, this polynomial is zero since:

2. The function $O(s)$ satisfies Watson's theorem:

$$\frac{O(s+i\epsilon)}{O(s-i\epsilon)} = e^{2i\delta(s)} = \frac{f^+(s+i\epsilon)}{f^+(s-i\epsilon)}, \quad s > s_{\text{th}} \quad (\text{A4})$$

Performing $n+1$ subtractions, one can produce a rank $n+2$ polynomial in the denominator of the dispersive integral of Eq. (A1). Indeed, for $s \notin L$

$$f^+(s) = P_n(s) + \frac{(s-s_0)(s-s_1)\cdots(s-s_n)}{\pi} \int_{s_{\text{th}}}^{+\infty} \frac{dx}{(x-s_0)(x-s_1)\cdots(x-s_n)} \frac{\text{Im}f^+(x)}{x-s}, \quad s_0, \dots, s_n < s_{\text{th}} \quad (\text{A5})$$

with the rank n polynomial $P_n(s)$ determined by the $n+1$ equations $P_n(s_i) = f^+(s_i)$, $i = 0, 1, \dots, n$,

$$P_n(s) = \sum_{j=0}^n \alpha_j(s) f^+(s_j), \quad \alpha_j(s) = \left[\prod_{j \neq k=0}^n \frac{s-s_k}{s_j-s_k} \right] \quad (\text{A6})$$

Note that $\alpha_j(s)$ are rank n polynomials, which satisfy

$$\sum_{j=0}^n \alpha_j(s) = 1 \quad (\text{A7})$$

On the other hand for $s > s_{\text{th}}$, we have from Eq. (17)

$$\log f^+(s+i\epsilon) - \log f^+(s-i\epsilon) = \log \frac{f^+(s+i\epsilon)}{f^+(s-i\epsilon)} = 2i\delta(s) = 2i\text{Im} [\log f^+(s+i\epsilon)] \quad (\text{A8})$$

Thus in analogy to Eq. (A5), assuming that the form factor does not vanish in $\mathcal{C} - \{s_{\text{th}}\}$ ¹⁵, or neglecting the contribution from the log cut if it has a finite branch point different from s_{th} , we can write

$$\log f^+(s) = \widehat{P}_n(s) + \frac{(s-s_0)(s-s_1)\cdots(s-s_n)}{\pi} \int_{s_{\text{th}}}^{+\infty} \frac{dx}{(x-s_0)(x-s_1)\cdots(x-s_n)} \frac{\delta(x)}{x-s}, \quad s \notin L \quad (\text{A9})$$

with

$$\widehat{P}_n(s) = \sum_{j=0}^n \alpha_j(s) \log f^+(s_j) \quad (\text{A10})$$

From the above equation one readily finds the $(n+1)$ -subtracted Omnès representation given in Eq. (16).

Finally, we would like to draw the reader's attention to a subtle point. In Eq. (A1) we have assumed that f^+ has no poles. However we know that if the scattering amplitude has a pole at $s_R = M_R^2 - iM_R\Gamma_R$ on its second Riemann sheet (resonance) or on the physical sheet (bound state with $\Gamma_R = 0^+$ and $M_R^2 < s_{\text{th}}$), it might show up as a pole in the complex plane of f^+ (see Eq. (12)). On the other hand, the S -matrix depends on $\exp(2i\delta)$, and thus one has the freedom to add factors of $m\pi$, for m an integer, to the phase-shift without modifying the S -matrix. However, the Omnès representation of the form factor will definitely depend on the specific value chosen for the integer m .

¹⁵ Note that, we have already treated $s = s_{\text{th}}$ as a branch point.

To fix this ambiguity, we will assume that at threshold the phase shift should be $\delta(s_{\text{th}}) = n_b\pi$, where n_b is the number of bound states in the channel, while $\delta(\infty) = k\pi$, where k is the number of zeros of the scattering amplitude on the physical sheet (this is Levinson's theorem [47]). This choice for the phase shifts also takes into account the existence of poles in the scattering matrix. We demonstrate with a simple example in which a p -wave T -matrix is proportional to $(s - s_{\text{th}})/(s - M_R^2 + iM_R\Gamma_R)$. The phase shift is given by

$$\delta(s) = \pi + \text{Arctan} \left[\frac{-M_R\Gamma_R}{s - M_R^2} \right], \quad s > s_{\text{th}} \quad (\text{A11})$$

with $\text{Arctan} \in [-\pi, \pi[$. This satisfies $\delta(\infty) = \pi$ and, if $M_R\Gamma_R \ll |s - M_R^2|$, it also leads to $\delta(s_{\text{th}}) = \pi$ or 0 for a bound state or resonance respectively, in accordance with Levinson's theorem. For simplicity, let us also assume $\Gamma_R \ll M_R$. In this circumstance we can approximate

$$\delta(s) \approx \pi [1 - H(M_R^2 - s)] = \pi H(s - M_R^2) \quad (\text{A12})$$

where $H(\cdot)$ is the step function. Since

$$\frac{s - s_0}{\pi} \int_{s_{\text{th}}}^{+\infty} \frac{dx}{x - s_0} \frac{\delta(x)}{x - s} \approx (s - s_0) \int_{\text{Max}(s_{\text{th}}, M_R^2)}^{+\infty} \frac{dx}{x - s_0} \frac{1}{x - s} = \log \left\{ \frac{\text{Max}(s_{\text{th}}, M_R^2) - s_0}{\text{Max}(s_{\text{th}}, M_R^2) - s} \right\}, \quad (\text{A13})$$

we find that the Omnès solution from a once-subtracted dispersion relation, Eq. (A2), reads

$$O(s) \approx f^+(s_0) \frac{\text{Max}(s_{\text{th}}, M_R^2) - s_0}{\text{Max}(s_{\text{th}}, M_R^2) - s} \quad (\text{A14})$$

It has a pole at $s = M_R^2$ for a resonance or at $s = s_{\text{th}}$ in the case of a bound state. For the case of a resonance with a finite width, the pole will move to $s = M_R^2 + iM_R\Gamma_R$. On the other hand, for a bound state, going beyond the approximation $\delta(s) \approx \pi$ (see Eq. (18)), the form factor will be sensitive to the exact position of the pole ($s = M_R^2$), since the effective range parameters (scattering volume, ...) will depend on M_R .

These conclusions can easily be generalized when a multiply-subtracted Omnès dispersion relation is used.

-
- [1] Particle Data Group, S. Eidelman et al., Phys. Lett. **B592** (2004) 1.
 - [2] CLEO Collaboration, J.P. Alexander et al., Phys. Rev. Lett. **77** (1996) 5000.
 - [3] CLEO Collaboration, S.B. Athar et al., Phys. Rev. **D68** (2003) 072003.
 - [4] UKQCD Collaboration, D.R. Burford et al., Nucl. Phys. **B447** (1995) 425.
 - [5] UKQCD Collaboration, L. Del Debbio, J.M. Flynn, L. Lellouch and J. Nieves, Phys. Lett. **B416** (1998) 392.
 - [6] S. Hashimoto et al., Phys. Rev. **D58** (1998) 014502-1; S. Aoki et al., Phys. Rev. **D64** (2001) 114505.
 - [7] UKQCD Collaboration, K.C. Bowler et al., Phys. Lett. **B486** (2000) 111.
 - [8] A. Abada et al., Nucl. Phys. **B619** (2001) 565.
 - [9] A. X. El-Khadra et al., Phys. Rev. **D64** (2001) 014502.
 - [10] HPQCD Collaboration, J. Shigemitsu, *hep-lat/0408019*.
 - [11] Fermilab Lattice Collaboration, M. Okamoto, *hep-lat/0409116*.
 - [12] P. Ball and V. M. Braun, Phys. Rev. **D58** (1998) 094016; P. Ball, JHEP **09** (1998) 005; P. Ball and R. Zwicky, JHEP **10** (2001) 019.
 - [13] A. Khodjamirian et al., Phys. Rev. **D62** (2000) 114002.
 - [14] Y.L. Wu and W.Y. Wang, Phys. Lett. **B515** (2001) 57; W.Y. Wang, Y.L. Wu and M. Zhong, Phys. Rev. **D67** (2003) 014024.
 - [15] J.G. Körner, C. Liu and C.T. Yan, Phys. Rev. **D66** (2002) 076007.
 - [16] Z.G. Wang, M. Zhou and T. Huang, Phys. Rev. **D67** (2003) 094006.
 - [17] W. Wirbel, B. Stech and M. Bauer, Z. Phys. **C29** (1985) 637; J. G. Körner and G.A. Shuler, Z. Phys. **C38** (1988) 511.
 - [18] N. Isgur, D. Scora, B. Grinstein and M.B. Wise, Phys. Rev. **D39** (1989) 799.
 - [19] N. Isgur and M.B. Wise, Phys. Rev. **D41** (1990) 151.
 - [20] D. Scora and N. Isgur, Phys. Rev. **D52** (1995) 2783.
 - [21] W. Jaus, Phys. Rev. **D41** (1990) 3394; *ibidem* **D53** (1996) 1349.
 - [22] I.L. Grach, I.M. Narodetskii and S. Simula, Phys. Lett. **385** (1996) 317.
 - [23] B. Stech, Z. Phys. **C75** (1997) 245; *ibidem* Phys. Lett. **B354** (1995) 447; D. Melikhov and B. Stech, Phys. Rev. **D62** (2000) 014006.
 - [24] A. Deandrea, R. Gatto, G. Nardulli and A.D. Polosa, Phys. Rev. **D61** (2000) 017502.

- [25] Riazuddin, T.A. Al-Aithan and A.H. Shah Gilani, *Int. Jour. Mod. Phys.* **A17** (2002) 4927.
- [26] R. Omnès, *Nuovo Cimento* **8** (1958) 316; N.I. Mushkelishvili, *Singular Integral Equations*, Noordhoff, Groningen, 1953.
- [27] J.M. Flynn and J. Nieves, *Phys. Lett.* **B505** (2001) 82.
- [28] J.M. Flynn and J. Nieves, *in preparation*.
- [29] C. Albertus, E. Hernández, J. Nieves and J.M. Verde-Velasco, *Phys. Rev.* **D71** (2005) 113006.
- [30] R. K. Bhaduri, L.E. Cohler, Y. Nogami, *Nuovo Cim.* **A65** (1981) 376.
- [31] B. Silvestre-Brac, *Few Body Systems* **20** (1996) 1.
- [32] F. Gutbrod and I. Montway, *Phys. Lett.* **136B** (1984) 411.
- [33] M. Fabre de la Ripelle, *Phys. Lett.* **205B** (1988) 97.
- [34] C. Albertus, J.E. Amaro, E. Hernández and J. Nieves, *Nucl. Phys.* **A740** (2004) 333.
- [35] C. Albertus, E. Hernández and J. Nieves, *Phys. Rev.* **D71** (2005) 014012.
- [36] S. Hashimoto, *hep-ph/0411126*.
- [37] M.B. Wise, *Phys. Rev.* **D45** (1992) R2188.
- [38] R. Casalbuoni et al., *Phys. Rep.* **281** (1997).
- [39] UKQCD Collaboration, K.C. Bowler et al., *Nucl. Phys.* **B619** (2001) 507.
- [40] A. Abada et al., *JHEP* **02** (2004) 016.
- [41] V.M. Belyaev, V.M. Braun, A. Khodjamirian and R. Rückl, *Phys. Rev.* **D51** (1995) 6177.
- [42] D. Becirevic and A. Le Yaouanc , *JHEP* **03** (1999) 021.
- [43] C. Bernard, et al., *Phys. Rev.* **D65** (2002) 014510.
- [44] V. Ciulli, *hep-ex/9911044*.
- [45] S. Mandelstam, *Phys. Rev.* **112** (1958) 1344.
- [46] K. M. Watson, *Phys. Rev.* **95** (1954) 228.
- [47] A.D. Martin and T.D. Spearman, *Elementary Particle Theory*, North-Holland, Amsterdam, 1970, p. 401.
- [48] E. Pallante and A. Pich, *Nucl. Phys.* **B592** (2001) 294.
- [49] J. Nieves and E. Ruiz-Arriola, *Phys. Lett.* **455** (1999) 30; *ibidem* *Nucl. Phys.* **A679** (2000) 57.
- [50] Fermilab, MILC and HPQCD Collaborations, C. Aubin et al., *Phys. Rev. Lett.* **94** (2005) 011601.
- [51] UKQCD Collaboration, K.C. Bowler et al., *Phys. Rev.* **D51** (1995) 4905.
- [52] BES Collaboration, M. Abilikhim, *Phys. Lett.* **B597** (2004) 39.
- [53] CLEO Collaboration, G.S. Huang et al., *Phys. Rev. Lett* **94** (2005) 011802.
- [54] CLEO Collaboration, A. Anastassov et al., *Phys. Rev.* **D65** (2002) 032003.
- [55] A. Abada et al., *Phys. Rev.* **D66** (2002) 074504.
- [56] FOCUS Collaboration, J.M. Link et al., *Phys. Lett.* **B607** (2005) 233.
- [57] P. Colangelo and F. De Fazio, *Phys. Lett.* **B532** (2002) 193.
- [58] MILC Collaboration, C. Aubin et al., *Phys. Rev.* **D70** (2004) 114501.